Fireside Corrosion of Alloys for USC Plants

K. Natesan, J. -H. Park, and D. L Rink
Argonne National Laboratory, 9700 South Cass Avenue, Argonne, IL 60439
E-mail: natesan@anl.gov; Telephone: (630) 252-5103; Fax: (630) 252-8681

Abstract

A program on fireside corrosion, in support of ultrasupercritical (USC) plants, is being conducted at Argonne National Laboratory to evaluate the performance of several structural alloys in the presence of mixtures of synthetic coal ash, alkali sulfates, and alkali chlorides. Experiments in the present program address the effects of deposit chemistry, temperature, and alloy chemistry on the corrosion response of alloys at temperatures in the range of 650-800°C. Fe-base materials selected for the study included intermediate-Cr ferritic and high-Cr austenitic alloys. Ni-base alloys selected for the study included 600, 601, 617, 690, 625, 602CA, 214, 230, 45TM, HR160, 740, and 693. Data were obtained on weight change, scale thickness, internal penetration, microstructural characteristics of corrosion products, mechanical integrity of the scales, and cracking of scales. The intermediate-Cr ferritic steels exhibited catastrophic corrosion at 650°C in the presence of 150-300 vppm NaCl in the exposure environment. Based on acquired corrosion information, we have proposed a mechanism for accelerated corrosion in the presence of a NaCl-containing oxidizing environment. We have modified the chemical composition of the surface of these alloys to improve their corrosion resistance in the fireside environment. The surface-modified alloys showed substantial resistance to corrosion after 200-h exposures. Additional tests are in progress to evaluate the long-term performance and the effect, if any, of the combination of ash and NaCl in the corrosion resistance of intermediate-Cr steels. Experiments are also underway to evaluate austenitic Fe- and Ni-base alloys in similar environments.

Background

Conceptual designs of advanced combustion systems that utilize coal as a feedstock must include improved thermal efficiency and significant reduction in release of sulfur oxides, nitrogen oxides, and carbon dioxide. Such systems require materials and components that can operate at much higher temperatures than those found in current coal-fired power plants. Component reliability and long-term, trouble-free performance of structural materials for these systems necessitate development/evaluation of materials in simulated coal-combustion environments. Apart from the environmental aspects of the effluent from coal combustion, one concern from the systems standpoint is the aggressiveness of the combustion environment toward boiler structural components, such as steam superheaters and reheaters.

Recently, the U.S. Department of Energy has started to reevaluate coal-fired steam generation plants and, in particular, the designs based on supercritical and ultrasupercritical steam conditions. The ultimate goal of the staged development of power systems is to change steam pressure and temperature from the current values of 16.5-24 MPa (2400-3500 psig) and 540°C (1000°F), respectively, to 34.5 MPa (5000 psig) and 650°C (1200°F). Development of a

revolutionary boiler design for U.S. markets, based on superheater/reheater temperatures >760°C, has been proposed. The higher steam temperature is expected to lead to another 2-3% increase in efficiency over a 700°C design, thus improving fuel usage and diminishing CO_2 emissions [1].

Fireside metal wastage in conventional coal-fired boilers can occur by gas-phase oxidation or deposit-induced liquid-phase corrosion. The former can be minimized by using materials which are resistant to oxidation at the service temperatures of interest. The latter is an accelerated type of attack, influenced by the vaporization and condensation of small amounts of impurities such as sodium, potassium, sulfur, chlorine, and vanadium (or their compounds) that are present in the coal feedstock. At the temperatures of interest in advanced combustion systems, mixtures of alkali sulfates, and alkali chlorides, dominate fireside deposit, and viable structural alloys must be resistant to attack by such deposits.

In advanced combustion systems, alkali sulfate and coal ash will be the predominant deposit because the metals in the superheater regions will be subjected to a much higher steam temperature. Several factors (including sulfur, alkali, and chlorine in coal feedstock; excess air level during the combustion process; and metal temperature dictated by the steam temperature) determine the extent of corrosion of superheater materials in coal-fired boilers. The objective of the present work is to evaluate the corrosion performance of state-of-the-art candidate materials in coal ash, alkali sulfate, and alkali chloride environments at temperatures in the range of 650-800°C. The goal of the experimental program is to develop a scientific understanding of corrosion mechanisms as a function of alloy composition and deposit chemistry, and to quantitatively determining the scaling and internal penetration of the alloys.

Experimental Procedure

Materials

Numerous alloys, both ASME coded and uncoded, were selected for corrosion evaluation. The advanced ferritic alloys included modified 9Cr, E 911, HCM 12A, and NF 616. These alloys contain varying amounts of W, Nb, M, and V, and are designed to improve the creep strength for service at temperatures up to 650°C. The compositions of the Fe-base alloys selected for the study are listed in Table 1. The included austenitic alloys were broadly based on 18-20Cr and 20-25Cr steels. Super 304H, 347HFG, and NF709 fall into 18-20Cr steels, with improved creep strength achieved by addition of Nb and/or Ti. HR3C, 310TaN, and SAVE 25 fall into 20-25Cr steels, with improved creep strength achieved by addition of Nb, Ti, Ta, and N. Modified 800 contains the Alloy 800 base, with additions of the strengthening elements Nb, V, N, and B. HR120 is a Fe-Ni-Cr alloy with additions of Co, W, N, and Nb. Specimens of 800H clad with Alloy 671 were also included in the study.

Table 2 lists the Ni-base alloys selected for the corrosion study. The alloys included 600, 601, 690, 617, 625, 602CA, 214, 230, 45TM, HR 160, and 693. Among them, Alloy 600 and 214 contained 15.4 and 15.9 wt.% Cr, respectively, whereas all of the others contained Cr in a range of 21.5-28.8 wt.%. In addition, Alloys 617 and 625 contained a high concentration of Mo; Alloys 601, 602CA, and 214 contained Al concentration in a range of 1.4-3.7 wt.%; and Alloys 45TM and HR 160 contained Si in a range of 2.7-2.8 wt.%.

Table 1. Nominal composition (in wt.%) of Fe-base alloys selected for corrosion study

Material	C	Cr	Ni	Mn	Si	Mo	Fe	Other
Modified 9Cr	0.10	9	0.8	0.5	0.4	1.0	Bal	Nb 0.08, V 0.20, N 0.06
E 911	0.12	9	0.3	0.5	0.2	0.9	Bal	W 0.9, V 0.2, Nb 0.06, N 0.06
NF 616	0.10	9	0.1	0.5	0.1	0.5	Bal	W 1.8, V 0.20
HCM12A	0.10	12	0.3	0.5	0.3	0.4	Bal	W 2.0, V 0.2, Nb 0.05, Cu 0.9, N 0.05
Super 304H	0.10	18	9	1.0	0.3	-	Bal	Nb 0.45, Cu 3.0, N 0.09
347HFG	0.08	18	11	2.0	1.0	-	Bal	Nb + Ta = 10 x C minimum
HR3C	0.06	25	20	1.2	0.4	-	Bal	Nb 0.45, N 0.2
310TaN	0.05	25	20	1.0	0.2	-	Bal	Ta 1.5, N 0.2
NF709	0.07	20	25	1.0	0.6	1.5	Bal	Ti 0.6, Nb 0.2, N 0.18, B 0.004
SAVE 25	0.10	23	18	1.0	0.4	-	Bal	Nb 0.45, W 1.5, Cu 3.0, N 0.2
Modified 800H	0.10	20	30	1.5	0.2	1.5	Bal	Ti 0.25, Nb 0.25, V 0.05, N 0.03, B 0.004
HR120	0.05	25	37	0.7	0.6	2.5	Bal	Co 3, W 2.5, N 0.2, Cu, Al 0.1, Nb 0.7
MA956	-	20	-	-	-	-	Bal	Al 4.5, Ti 0.5, Y_2O_3 0.6
671-clad 800H								
671	0.05	48	Bal	0.02	0.2	-	0.2	Ti 0.4
800H	0.05	21	32	0.5	0.2	-	Bal	Ti 0.4, Al 0.4

Table 2. Nominal composition (in wt.%) of Ni-base alloys selected for corrosion study

Material	C	Cr	Ni	Mn	Si	Mo	Fe	Other
600	0.04	15.4	Bal	0.2	0.1	-	9.7	-
601	0.03	21.9	Bal	0.2	0.2	0.1	14.5	Al 1.4, Ti 0.3, Nb 0.1
690	0.01	27.2	61.4	0.2	0.1	0.1	10.2	Ti 0.3, Al 0.2
617	0.08	21.6	53.6	0.1	0.1	9.5	0.9	Co 12.5, Al 1.2, Ti 0.3
IN 625	0.05	21.5	Bal	0.3	0.3	9.0	2.5	Nb 3.7, Al 0.2, Ti 0.2
602CA	0.19	25.1	62.6	0.1	0.1	-	9.3	Al 2.3, Ti 0.13, Zr 0.19, Y 0.09
214	0.04	15.9	Bal	0.2	0.1	0.5	2.5	Al 3.7, Zr 0.01, Y 0.006
230	0.11	21.7	60.4	0.5	0.4	1.4	1.2	W 14, Al 0.3, La 0.015
45TM	0.08	27.4	46.4	0.4	2.7	-	26.7	Rare earths 0.07
HR 160	0.05	28.0	Bal	0.5	2.8	0.1	4.0	Co 30, Al 0.2
693	0.02	28.8	Bal	0.2	0.04	0.13	5.8	Al 3.3, Nb 0.67, Ti 0.4, Zr 0.03

Corrosion in NaCl-containing environments

In earlier studies of corrosion of Fe-based alloys in simulated fireside environments, the presence of low concentrations (≈1 wt.%) of NaCl in the ash deposit led to significant acceleration of the corrosion process and high metal wastage [2-4]. To examine the role of NaCl vapor (arising from combustion of coal) during the corrosion process, several corrosion experiments were conducted at 650°C with the four intermediate-chromium ferritic steels in an air-1 vol% SO_2 environment that contained 300 ppm NaCl. The experimental setup (see Fig. 1) consisted of a resistance-wound furnace in which an alumina tube was inserted as the reaction chamber. The concentration of NaCl for the test was calculated from the temperature dependence of vapor pressure of NaCl vapor; the required amount of NaCl for the test was determined from vaporization curves (see Fig. 2). Corrosion tests are in progress on Ni- and Fe-base austenitic alloys in air-1 % SO_2 and in pure argon environments with and without addition of 300 ppm NaCl. To evaluate the role of NaCl in the corrosion mechanism and in

the cause for accelerated corrosion of these alloys, each test was conducted for 100 h at 650°C.

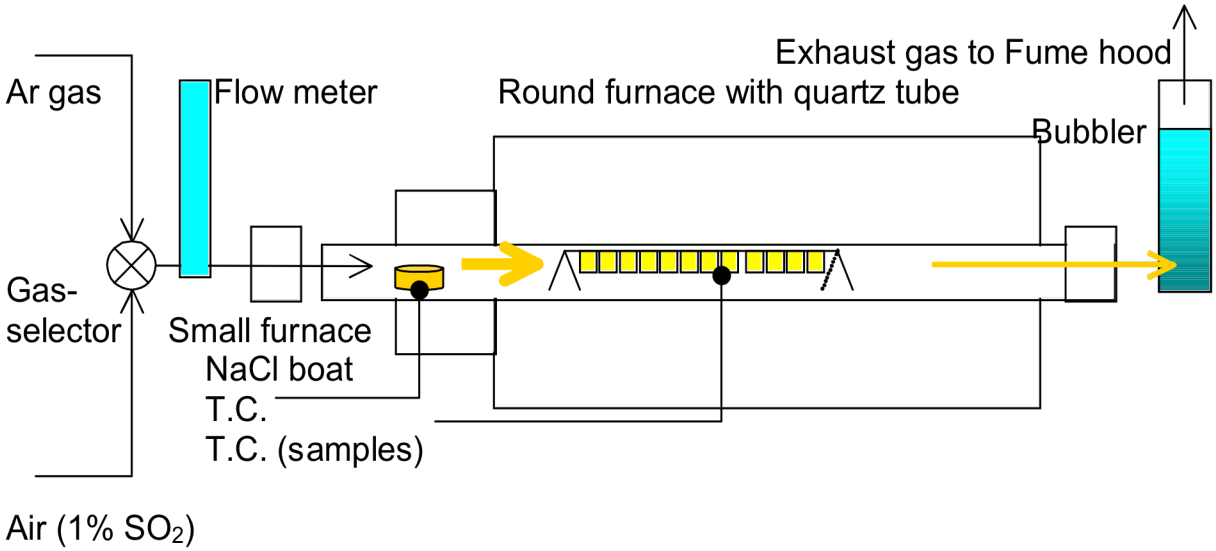

Figure 1. Schematic representation of setup for of corrosion experiments.

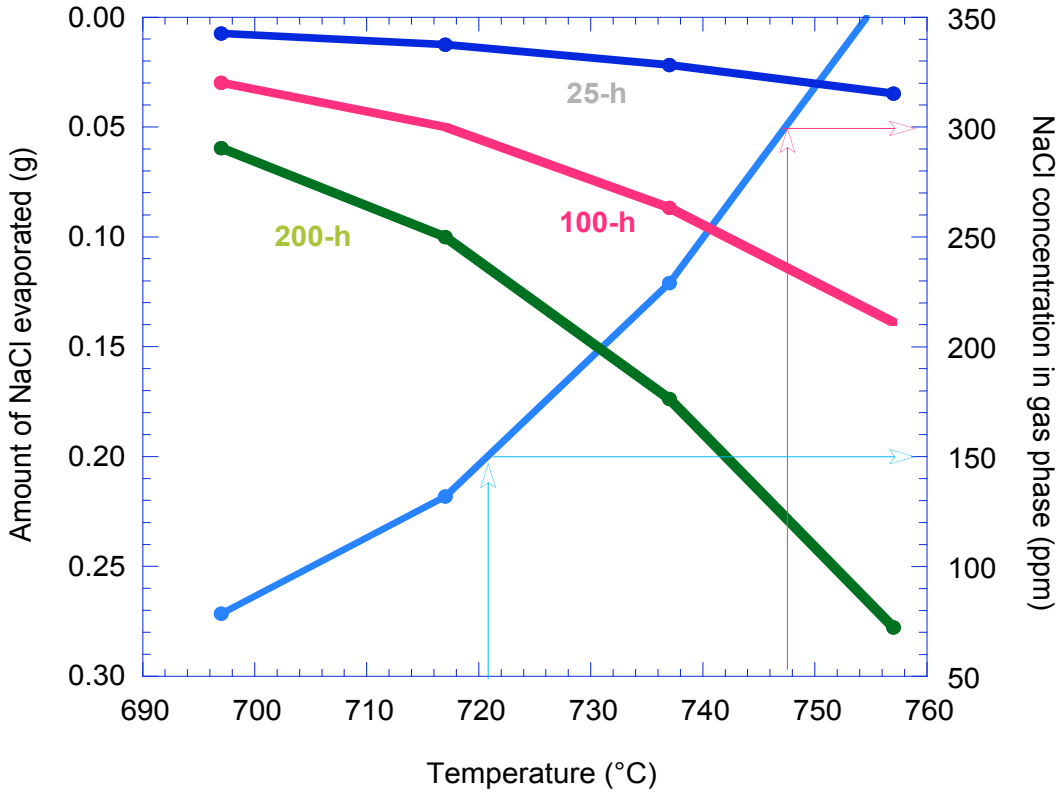

Figure 2. NaCl vaporization curves.

Results and Discussion

Scaling Kinetics and Corrosion Morphology

The specimens that were exposed to an air-1% SO_2 gas mixture that contained 300 ppm NaCl exhibited very friable oxide scales with significant spalling (see Fig. 3). Figure 4 shows a typical scanning electron microscopy (SEM) photomicrograph of the cross section of one of the ferritic alloys after a 100-h exposure at 650°C. The scale thickness in these alloys ranged between 400 and 600 µm after a 100-h exposure. It is evident that the rapid growth rate of the scale and significant spallation do not offer oxidation protection for these alloys, even though the scale is predominantly iron-rich oxide.

Experiments were also conducted with these alloys in other environments, such as air-1% SO_2 (no NaCl) and argon-300 ppm NaCl (no oxygen), at 650°C for 100 h. Figure 5 shows the observed weight change for the four alloys in the three environments

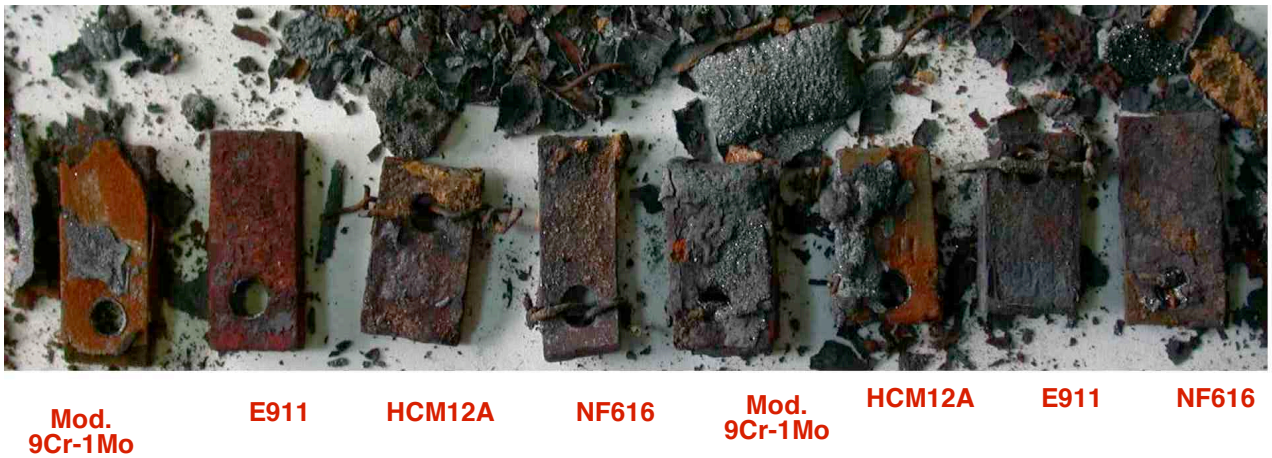

Figure 3. Photograph of duplicate specimens of intermediate-chromium ferritic alloys after 100-h exposure at 650°C to air-1% SO_2 environment containing 300 ppm NaCl.

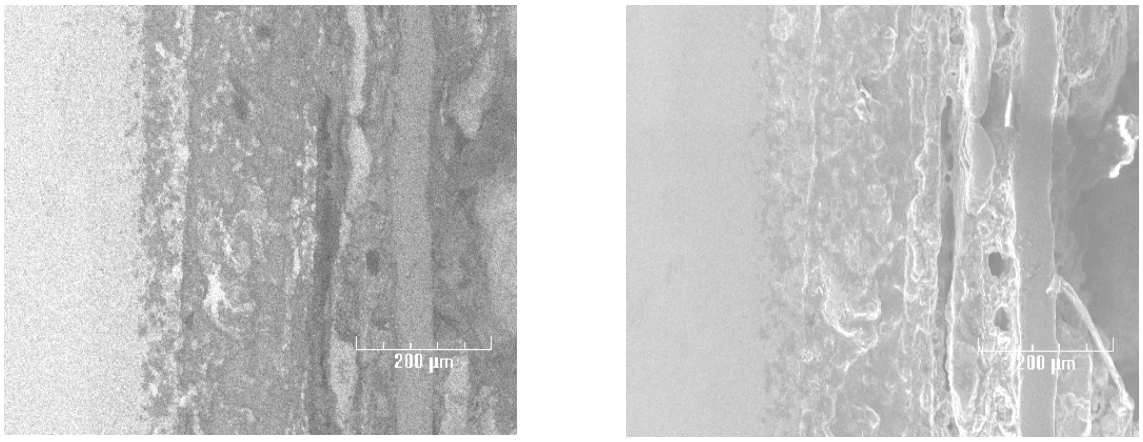

Figure 4. Typical SEM photomicrographs of cross section of intermediate-chromium steel after 100-h exposure at 650°C to an air-1% SO_2 environment containing 300 ppm NaCl. Left: Back scattered electron image and Right: Secondary electron image.

after a 100-h exposure. In both air-1%SO_2 and argon-300 NaCl environments, all three alloys developed thin adherent oxide scales and the weight changes were negligibly small. The data in Fig. 5 also indicates that the simultaneous presence of oxygen and NaCl leads to orders of magnitude increase in scale growth rate that leads to spallation of the scales. We have conducted similar experiments in an air-1% SO_2 environment that contained 150 ppm NaCl and observed similar behavior. A detailed analysis of the physical characteristics of the scales developed in the presence of NaCl showed that the scales were dense, with almost no porosity. Furthermore, the concave shape of the scales (see the detached scale in the center of Fig. 3) indicates that the scale is pushed away from the substrate, probably by a volatile species at the scale/metal interface.

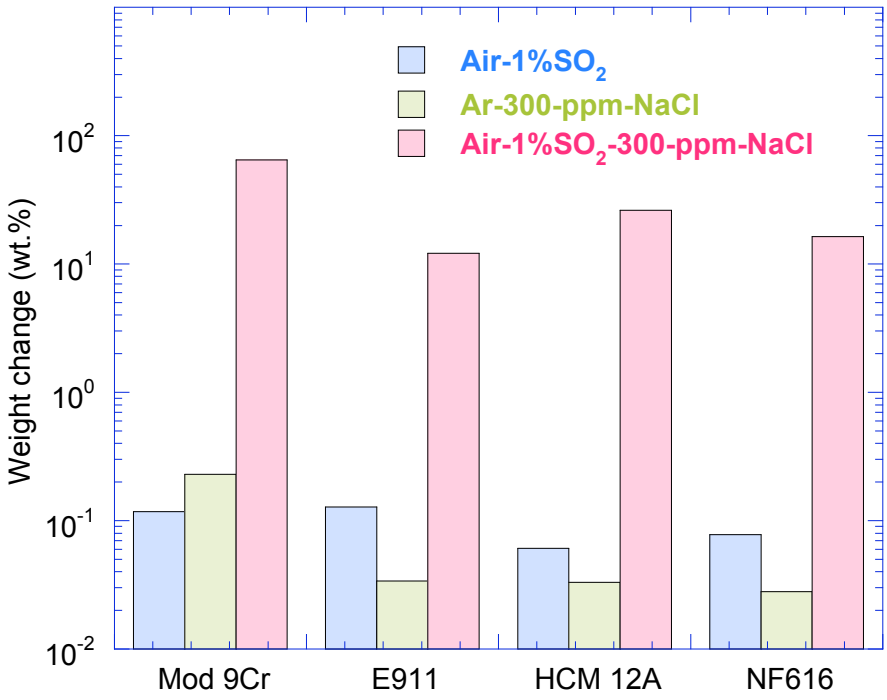

Figure 5. Weight change data for four intermediate-chromium steels after 100-h exposure in three environments at 650°C.

Corrosion Mechanism

The cause of the accelerated corrosion in the heat-resistant alloys in the presence of NaCl is twofold: the NaCl in the vapor phase establishes a Cl activity, which can attack the carbides that are present in the alloy as strengtheners; and the Cl activity in the deposit near the alloy can be high enough to form volatile chlorides of Fe, Cr, and Al (if present in the alloy). The volatile chlorides can lead to a microstructure conducive to continued transport of Cl from the gas phase to the alloy substrate.

Based on our experiments, the corrosion rates for the intermediate-Cr ferritic steels is accelerated by the simultaneous presence of compounds that contained Cl and gas phase oxygen. Even though these alloys develop iron oxide scales, the NaCl from the vapor phase deposits on the oxide surface and thereby incorporates the sodium ions on the iron sites and the

chlorine ions on the oxygen sublattice. Table 3 lists the charge and ionic radii of elements of interest for the scaling and deposition processes. The reactions of interest are

$$Na^{+} + V_{Fe}'' + 2h^{\bullet} \Rightarrow Na_{Fe}' + 2h^{\bullet}$$

and

$$Cl^{-} + O_{O}^{X} \Rightarrow Cl_{O}^{\bullet} + 2e' + \tfrac{1}{2} O_2 (g)$$

Table 3. Ionic radii of elements of interest for scaling and deposition processes

Element	Charge	Ionic radius (Å)
Na	+1	0.97
Cl	-1	1.81
Fe	+2	0.74
	+3	0.64
O	-2	1.32

The point defects in iron oxide in a high-pO_2 environment are based on the reaction

$$FeO \Rightarrow O_{O}^{X} + V_{Fe}'' + 2h^{\bullet}$$

Scale growth occurs by cation diffusion outwards and the doubly charged iron vacancies are generated at the outer scale, and iron vacancies and electron holes migrate inward as ambipolar transport. At the scale/gas interface, the V_{Fe}'', $h^{\bullet}$, Na_{Fe}', and $Cl_{O}^{\bullet}$ are the major defect species responsible for the growth of the scale. No sodium specie was detected in our analysis of the inner scale of specimens exposed to NaCl-containing environment; therefore, inward diffusion of sodium can be ignored. Because the sodium ions with a negative charge are located in the iron sublattice, their transport will be determined by the competition from inward-diffusing doubly ionized iron vacancies. The chlorine ions on the oxygen sublattice at the scale/gas interface can be considered positively charged point defects, $Cl_{O}^{\bullet}$. In as much as the negatively charged iron vacancies migrate inwards, the electron holes and/or positively charged $Cl_{O}^{\bullet}$ act as a counter component part of the ambipolar diffusion process. The activity of $Cl_{O}^{\bullet}$ will be dictated by the concentration of NaCl in the gas phase. The chlorine that is transported inwards can lead to iron chloride at the scale/substrate interface. The high vapor pressure of iron chloride is one of the critical factors for accelerating the corrosion of these steels in chlorine-containing environments. Generation of iron cations at the substrate by the reaction, $Fe \Rightarrow Fe^{2+} + 2e'$ is accelerated by the presence of chlorine due to the large electron affinity (EA) of chlorine and/or iron chloride(s), as shown in Fig. 6.

Avenues for Corrosion Protection

Based on the results we have generated on the corrosion of ferritic steels in a NaCl-containing oxidizing environment and on the possible mechanism for the accelerated corrosion (discussed above, the primary means to control this form of degradation is to develop an approach that will

minimize the inward transport of chlorine. The attack can be minimized if the adsorption and dissociation of NaCl can be controlled or if a sink for chlorine (in the vicinity of scale/gas

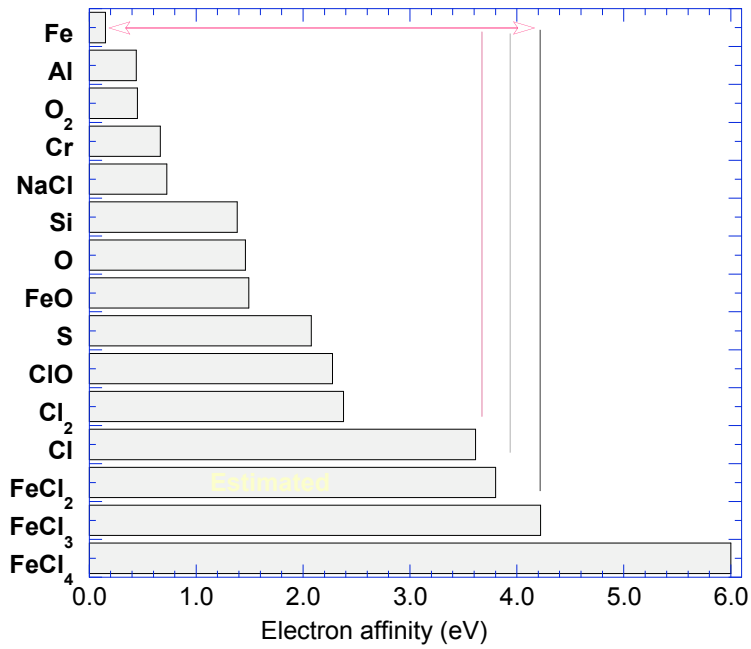

Figure 6. Electron affinity of various chemical species used to predict ionization of iron during accelerated chlorine-induced corrosion of ferritic steels.

interface) can be developed and thereby minimize inward transport of chlorine and subsequent reaction with the substrate alloy. With this objective, we have developed coatings for ferritic steels at relatively low temperatures to minimize chlorine transport. The coating procedure and other pertinent details are not discussed here because a patent application for the process is currently being filed. Briefly, we coated several specimens of the four intermediate-chromium ferritic steels and characterized the coatings in the as-coated condition. We have also exposed the coated specimens in an air-1%SO_2-300 ppm NaCl environment for 100 and 200 h at 650°C (see Figs. 7 and 8).

Figure 7. Photograph of duplicate specimens of coated intermediate-chromium ferritic alloys after 100-h exposure at 650°C to air-1% SO_2 environment containing 300 ppm NaCl.

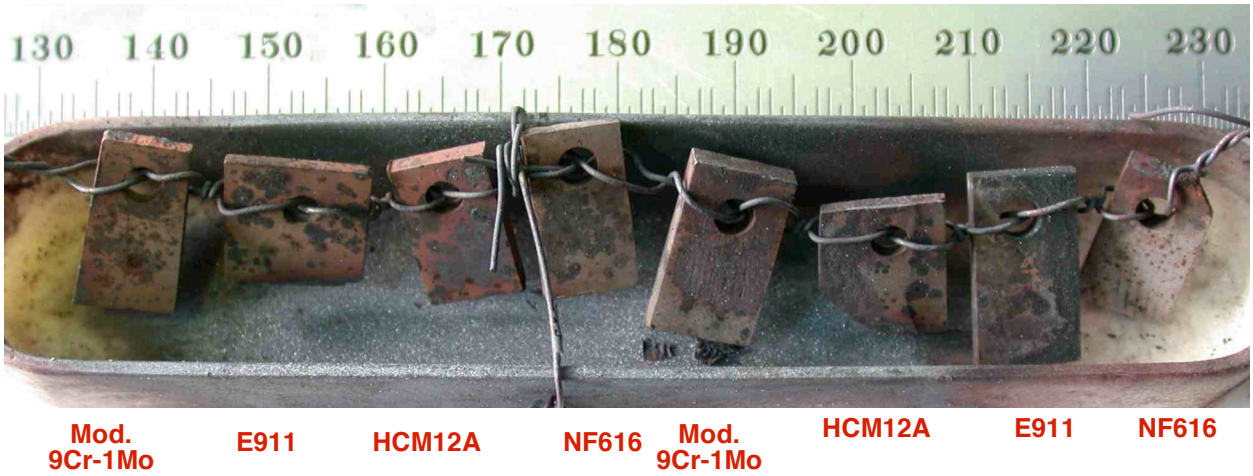

Figure 8. Photograph of duplicate specimens of coated intermediate-chromium ferritic alloys after 200-h exposure at 650°C to air-1% SO_2 environment containing 300 ppm NaCl.

We examined in detail the coated specimens after exposure to a NaCl-containing oxidizing environment. The results of short-term tests show substantial improvement in corrosion resistance. To evaluate coatings on intermediate-Cr steels, we plan to perform long-term tests and tests in the combined environment of coal ash and NaCl. In addition, similar tests in a NaCl-containing environment are in progress on several austenitic Fe- and Ni-base alloys.

Summary

Fireside and steam-side corrosion are major issues when selecting materials for advanced steam-cycle systems. At Argonne National Laboratory, we have conducted studies to evaluate the corrosion performance of candidate Fe- and Ni-base alloys in coal-ash and in steam environments. The laboratory tests simulate the combustion atmosphere of advanced steam-cycle systems and three deposit chemistries that included ash constituents, alkali sulfates, and NaCl.

Intermediate-Cr ferritic steels showed accelerated corrosion in the presence of oxidizing environments that contained 150-300 ppm NaCl. Based on the obtained test data, we have proposed a mechanism for Cl-induced corrosion in these steels. Subsequently, we developed a relatively low-temperature approach to modify the surface of these alloys to minimize chlorine transport through the oxide scale and thereby decrease the corrosion rate. Test data obtained after 200-h exposures showed substantial decrease in corrosion rate for the surface-modified alloys. Additional tests are in progress to evaluate the long-term performance and the effect, if any, of the combination of ash and NaCl in the corrosion resistance of intermediate-Cr steels. Experiments are also underway to evaluate austenitic Fe- and Ni-base alloys in similar environments.

References

[1]. R. Viswanathan and W. Bakker, J. Mater. Eng. Perf. 10 (1), 2001, 81.

[2]. K. Natesan, A. Purohit, and D. L. Rink, Fireside Corrosion of Alloys for Combustion Power Plants, Proc. 16th Annual Conference on Fossil Energy Materials, Baltimore, MD, April 22-24, 2002.
[3]. K. Natesan, A. Purohit, and D. L. Rink, Coal-ash Corrosion of Alloys for Combustion Power Plants, Proc. 17th Annual Conference on Fossil Energy Materials, Baltimore, MD, April 22-24, 2003.
[4]. K. Natesan and D. L. Rink, Fireside and Steamside Corrosion of Advanced Steam-Cycle Materials, Proc. 18th Annual Conference on Fossil Energy Materials, Knoxville, TN, June 2-4, 2004.

Acknowledgment

This work was supported by the U.S. Department of Energy, Office of Fossil Energy, Advanced Research Materials Program, Work Breakdown Structure Element ANL–4, under Contract W–31–109–Eng–38.